

Document downloaded from:

<http://hdl.handle.net/10251/58697>

This paper must be cited as:

Arrieta, MP.; López Martínez, J.; Rayón Encinas, E.; Jiménez, A. (2014). Disintegrability under composting conditions of plasticized PLA-PHB blends. *Polymer Degradation and Stability*. 108:307-318. doi:10.1016/j.polymdegradstab.2014.01.034.



The final publication is available at

<http://dx.doi.org/10.1016/j.polymdegradstab.2014.01.034>

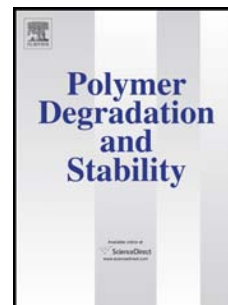
Copyright Elsevier

Additional Information

Accepted Manuscript

Disintegrability under composting conditions of plasticized PLA-PHB blends

M.P. Arrieta, J. López, E. Rayón, A. Jiménez



PII: S0141-3910(14)00045-7

DOI: [10.1016/j.polymdegradstab.2014.01.034](https://doi.org/10.1016/j.polymdegradstab.2014.01.034)

Reference: PDST 7237

To appear in: *Polymer Degradation and Stability*

Received Date: 26 November 2013

Revised Date: 20 January 2014

Accepted Date: 26 January 2014

Please cite this article as: Arrieta MP, López J, Rayón E, Jiménez A, Disintegrability under composting conditions of plasticized PLA-PHB blends, *Polymer Degradation and Stability* (2014), doi: 10.1016/j.polymdegradstab.2014.01.034.

This is a PDF file of an unedited manuscript that has been accepted for publication. As a service to our customers we are providing this early version of the manuscript. The manuscript will undergo copyediting, typesetting, and review of the resulting proof before it is published in its final form. Please note that during the production process errors may be discovered which could affect the content, and all legal disclaimers that apply to the journal pertain.

Disintegrability under composting conditions of plasticized PLA-PHB blendsArrieta, M.P.^{a,b,*}, López, J.^a, Rayón, E.^c, Jiménez, A.^d^aInstituto de Tecnología de Materiales. Universitat Politècnica de Valencia, E-03801, Alcoy-

Alicante, Spain. marrieta@itm.upv.es

^bCatholic University of Cordoba, Camino a Alta Gracia Km 7½, 5017 Córdoba, Argentina.^cInstituto de Tecnología de Materiales. Universitat Politècnica de Valencia, E-46022, Valencia, Spain.^dAnalytical Chemistry, Nutrition and Food Sciences Department. University of Alicante, E-03080, Alicante, Spain.

The disintegration under composting conditions of films based on poly(lactic acid)-poly(hydroxybutyrate) (PLA-PHB) blends and intended for food packaging was studied. Two different plasticizers, poly(ethylene glycol) (PEG) and acetyl-tri-n-butyl citrate (ATBC), were used to limit the inherent brittleness of both biopolymers. Neat PLA, plasticized PLA and PLA-PHB films were processed by melt-blending and compression moulding and they were further treated under composting conditions in a laboratory-scale test at 58 ± 2 °C. Disintegration levels were evaluated by monitoring their weight loss at different times: 0, 7, 14, 21 and 28 days. Morphological changes in all formulations were followed by optical and scanning electron microscopy (SEM). The influence of plasticizers on the disintegration of PLA and PLA-PHB blends was studied by evaluating their thermal and nanomechanical properties by thermogravimetric analysis (TGA) and the nanoindentation technique, respectively. Meanwhile, structural changes were followed by Fourier transformed infrared spectroscopy (FTIR). The ability of PHB to act as nucleating agent in PLA-PHB blends slowed down the PLA disintegration, while plasticizers speeded it up. The relationship between the mesolactide to lactide forms of PLA was calculated with a Pyrolysis-Gas Chromatography-Mass Spectrometry device (Py-GC/MS), revealing that the mesolactide form increased during composting.

Keywords: Poly(lactic acid); Poly(hydroxybutyrate); blend; biodegradable; plasticizers.

*Corresponding author. Tel.: +34-966528433; fax: +34-966528433

E-mail address: marrieta@itm.upv.es (M.P. Arrieta)

1- Introduction

35

36

37

38

39

40

41

42

43

44

45

46

47

48

49

50

51

52

53

54

55

56

57

58

59

60

61

62

63

64

65

66

67

68

Poly(lactic acid), PLA, and poly-hydroxybutyrate (PHB) are two of the bio-based and biodegradable polymers which have focused some attention by their possibilities as environmentally-friendly food packaging materials. In this sense, PLA is currently the most used biopolymer in the food packaging sector for short shelf-life products [1-4], owing to its high mechanical strength, easy processability, superior transparency, availability and low cost. Poly(hydroxybutyrate) (PHB) is the most common representative of poly(hydroxyalkanoates) (PHA) [5], and it has been also proposed for short-term food packaging applications [6]. Conversely, there are not many commercial products of PHB by its narrow processing window, high brittleness, [5] and price [7].

A considerable number of research work has been reported on the miscibility between PLA and PHB and possible applications in food packaging [8-11] It is known that PLA shows limited or partial miscibility with low molar mass PHB [10, 12]. The temperature used during the blend preparation has also significant influence in the miscibility between both polymers. In this sense Zhang et al. (1996) reported that PLA-PHB blends prepared at high temperature exhibited greater miscibility than those prepared by solvent casting at room temperature [13] since PLA-PHB systems are fully miscible in the melt state [11, 14]. This effect could be due to the transesterification reaction between PLA and PHB chains [13]. In addition, the miscibility between PLA and PHB is strongly dependent on their ratio in the blend. For instance, Furukawa et al. (2005) studied PLA/PHB films prepared by solvent casting in chloroform with blending ratios (w/w) 20/80, 40/60, 60/40, and 80/20 (PLA/PHB). They reported that PHB crystallized as very small spherulites that may act as nucleation sites of PLA in the 20/80 blend [8]. Similarly, Zhang and Thomas (2011) studied PLA/PHB blends in different proportions (100/0, 75/25, 50/50, 25/75 and 0/100, w/w) prepared by melt blending followed by compression moulding [9]. They found that PLA/PHB 75/25 films showed interesting properties for specific applications, with increased crystallinity and optimal miscibility between both polymers, resulting in improved tensile properties compared with neat PLA. More recently, Bartczak et al. (2013) proposed the modification of PLA by the addition of PHB up to 20 wt% for food packaging applications and they concluded that PHB can be considered as an effective impact modifier for PLA, increasing its impact resistance [10]. PLA-PHB blends (75:25, w/w) prepared by melt-blending and compression moulding have been proposed for films intended for food packaging [3, 5] and it was observed that the addition of 25 wt% of PHB improved PLA mechanical and barrier properties due to the ability of PHB to act as a nucleating agent at this PLA/PHB ratio [5].

69 Films processed from PLA/PHB blends are still rigid and brittle, while their
70 processing for films manufacturing remains an issue to avoid fractures [5]. This drawback can
71 be overcome by plasticization to improve processability and ductility of these films [3, 5]. But
72 not all plasticizers could be adequate for such application. It should be taken into account that
73 plasticizers should satisfy the strict requirements applied to materials intended to be in contact
74 with food. They should be also miscible with the polymer matrix [1, 15, 16] and stable at the
75 high temperatures used during processing [16], providing suitable mechanical and barrier
76 properties [15]. In this sense, poly(ethylene glycol) (PEG) and citrate esters have been
77 proposed as efficient plasticizers for PLA [16, 17], while PHB has been successfully
78 plasticized with PEG [18] and acetyl-tri-n-butyl citrate (ATBC) [19]. PEG is water-soluble
79 [20] and ATBC is obtained from naturally occurring citric acid. Both are non-toxic
80 plasticizers [21].

81 These blends are promising candidates for sustainable post-use waste treatments, such
82 as composting [22]. Disintegration in compost is governed by aerobic fermentation that
83 mostly results in humus-rich soil, while landfill disposal is mediated by anaerobic
84 fermentation producing hazardous methane. Even if methane produced in landfills could be
85 used as an energy source [22], it is known that the huge amount of plastic waste disposal in
86 landfills must be reduced [23, 24]. Thus, composting would be adequate for short-term food
87 packaging plastics as end-life option.

88 Biodegradation in composting conditions of PLA [25-27] and PHB [5, 6] has been
89 already reported. It is known that PLA degradation in compost takes place in two main and
90 consecutive stages, i.e. the hydrolytic and enzymatic degradation [23]. PLA disintegration
91 starts by surface hydrolysis [28] leading to polymer random decomposition [4], while PHB
92 disintegration is firstly caused by microorganisms that erode the polymer surface and
93 gradually spreading to the bulk [29]. Lemmouchi et al. (2009) reported that the disintegration
94 of PLA in composting conditions was enhanced by the presence of plasticizers [5].

95 The influence of PHB and plasticizers on the PLA disintegrability in composting
96 conditions was evaluated in this work. Plasticized PLA/PHB films were prepared by melt-
97 blending followed by compression moulding. The disintegration patterns during composting
98 of plasticized PLA/PHB films were investigated and compared with their plasticized PLA
99 counterparts. Disintegrability was followed by morphological, structural, nanomechanical and
100 thermal analysis, with the main objective to obtain information on the compostability of
101 plasticized PLA-PHB blends as end-life option for food packaging applications.

2. Experimental

2.1. Materials

Poly(lactic acid) (PLA Ingeo™ 4032D, $M_n = 217$ kDa, 2 wt% D-isomer, $M_w / M_n = 2$) was supplied in pellets by NatureWorks LLC (Minnetonka, MIN, USA), Poly(hydroxybutyrate) pellets (PHB, P226, $M_w = 426$ kDa) was purchased from Biomer (Krailling, Germany). Poly(ethylene glycol) (PEG, $M_n = 300$ g mol⁻¹) and acetyl-tri-n-butyl citrate (ATBC, $M = 402$ g mol⁻¹, 98% purity) were purchased from Sigma-Aldrich (Madrid, Spain).

2.2. Films preparation

PLA-PHB blends were processed by mixing PLA (previously dried overnight at 80 °C in a vacuum oven) and PHB pellets (treated for 4 hours at 40 °C), in 75:25 wt% ratio in a Haake PolyLab QC mixer (Thermo Fischer Scientific Inc., Waltham, MA, USA) at 180 °C and a rotation speed of 50 rpm for 4 min. ATBC and PEG were further added (15 wt%) after 3 min once PLA or PLA-PHB blends had achieved the melt state. Each blend was then processed into films by compression moulding at 180 °C in a hot press (Mini C 3850, Carver, Inc., Wabash, IN, USA). Blends were kept between the plates at atmospheric pressure for 2 min until melting and they were further submitted to a pressure cycle of 3 MPa for 1 min, 5 MPa for 1 min and finally 10 MPa for 2 min, with the aim to eliminate the trapped air bubbles [30]. These films were then quenched to room temperature. Five formulations were obtained: control neat PLA film, PLA plasticized with PEG or ATBC (PLA-PEG and PLA-ATBC), and plasticized PLA-PHB blends (PLA/PHB-PEG and PLA/PHB-ATBC). The films average thickness, measured with a Digimatic Micrometer Series 293 MDC-Lite (Mitutoyo, Japan) \pm 0.001 mm, was 200 ± 50 μ m. Control films were stored at 25 °C and 30% relative humidity (RH) in an acrylic desiccator cabinet before testing.

2.3. Disintegration under composting conditions

Disintegration under composting conditions was performed by following the ISO-20200 standard [31]. Solid synthetic waste was prepared by mixing 10% of compost at pH 6.5 (supplied by Mantillo, Spain), 30% rabbit food, 10% starch, 5% sugar, 1% urea, 4% corn oil and 40% sawdust and it was mixed with water in 45:55 ratio. Water was added periodically to the reaction container to maintain the relative humidity in the compost medium. Films were prepared ($30 \times 30 \times 0.2$ mm³) and they were buried 6 cm depth in plastic reactors containing

137 the solid synthetic wet waste. Each sample was contained in an iron mesh to allow their easy
138 removal after treatment, but allowing the access of microorganisms and moisture [32].
139 Reactors were introduced in an air circulation oven (DO/200 Carbolite, Hope Valley, UK) at
140 58 °C for 35 days. The aerobic conditions were guaranteed by periodical gentle mixing of the
141 solid synthetic wet waste [18, 25]. Films were recovered from the disintegration container at
142 different times (7, 14, 21 and 28 days), washed with distilled water, dried in an oven at 37 °C
143 for 24 h, and weighed. Disintegrability was calculated by normalizing the sample weight at
144 each time to the initial value [33], while photographs were taken to all samples once extracted
145 from the composting medium.

146

147 2.4. Characterization techniques

148 2.4.1. Color properties

149 Color properties of plasticized PLA and plasticized PLA/PHB films before and after 7
150 days of incubation were studied by measuring CIELab colour coordinates L (lightness), a^*
151 (red-green) and b^* (yellow-blue), with a KONICA CM-3600d COLORFLEX-DIFF2,
152 HunterLab (Hunter Associates Laboratory, Inc, Reston, VA, USA) colorimeter. The
153 yellowness index (YI) was also determined. The instrument was calibrated with a white
154 standard tile. Measurements were carried out in quintuplicate at random positions over the
155 films surface and average values were calculated. Total color differences (ΔE) induced by
156 disintegration in samples after 7 days in composting conditions with the control films were
157 calculated by using Equation 1:

158

$$159 \Delta E = \sqrt{\Delta L^2 + \Delta a^{*2} + \Delta b^{*2}} \quad (1)$$

160

161 2.4.2. Surface microstructure

162 Differences in surface microstructures of plasticized PLA and plasticized PLA/PHB
163 films before and after 21 days of treatment were evaluated by using a LV-100 Nikon Eclips
164 optical microscope equipped with a Nikon sight camera at 20X magnification (Tokyo, Japan).
165 The extended depth of field (EDF-z) imaging technique was used to improve resolution.
166 Furthermore, surface microstructure of films before and after 14 and 21 days of disintegration
167 was studied by Scanning Electron Microscopy (SEM) with a Phenom (FEI Company,
168 Eindhoven, The Netherlands) operated at 10 kV.

169

170 2.4.3. Fourier transformed infrared spectroscopy (FTIR)

171 FTIR analysis of films was carried out in the 600-4000 cm^{-1} range in attenuated total
172 reflection (ATR) mode with a Perkin-Elmer BX IR spectrometer (Perkin Elmer Spain, S.L.,
173 Madrid Spain). Tests were performed at room temperature using 128 scans and 4 cm^{-1}
174 resolution. A background spectrum was obtained before each test to compensate by spectra
175 subtraction the humidity effect and the presence of carbon dioxide.

176

177 2.4.4. Thermogravimetric analysis (TGA)

178 Thermogravimetric analysis was performed with a thermogravimetric analyzer
179 TGA/SDTA-851e Mettler Toledo (Schwarzenbach, Switzerland). Tests were run under
180 dynamic mode from 30 to 600 $^{\circ}\text{C}$ at 10 $^{\circ}\text{C min}^{-1}$ in nitrogen flow (50 mL min^{-1}) to avoid
181 thermo-oxidative degradation. The initial degradation temperatures (T_0) were determined at
182 5% mass loss while temperatures at the maximum degradation rate (T_{max}) were calculated
183 from the first derivative of the TG curves (DTG).

184

185 2.4.5. Pyrolysis/ Gas Chromatography- Mass Spectrometry (Py/ GC-MS)

186 The relationship between mesolactide and (D, L)-lactide forms in the PLA structure
187 before and after 21 days under composting conditions was evaluated with a Pyrolysis-Gas
188 Chromatography-Mass Spectrometry device (Py-GC/MS). Film samples were pyrolyzed at
189 1000 $^{\circ}\text{C}$ for 0.5 s with a Pyroprobe 1000 (CDS Analytical, Oxford, PA, USA), coupled to a
190 gas chromatograph (6890N, Agilent Technologies, Spain S.L., Madrid, Spain) equipped with
191 a 30 m long HP-5 (0.25 mm thickness) column and using helium as carrier gas with a 50:1
192 split ratio. The GC oven was programmed as previously reported [34], the column program
193 started at 40 $^{\circ}\text{C}$ for 2 min, followed by a stepped increase of 5 $^{\circ}\text{C min}^{-1}$ to 200 $^{\circ}\text{C}$ (15 min
194 hold), and further increase at 20 $^{\circ}\text{C min}^{-1}$ to 300 $^{\circ}\text{C}$ (5 min hold). Detection was carried out
195 with an Agilent 5973N mass selective instrument. The transfer temperature from the GC to
196 the MS was set at 180 $^{\circ}\text{C}$. The mass selective detector was programmed to detect masses
197 between 30 and 650 amu. The identification of PLA and PHB degradation products was
198 carried out by the characteristic fragmentation patterns observed in Py-GC/MS spectra.

199

200 2.4.6. Nanomechanical properties

201 Nanomechanical properties were measured with a nanoindenter machine G-200
202 (Agilent Technologies, Santa Clara, CA, USA) with a previously calibrated Berkovich
203 diamond tip. Experiments were carried out by Continuous Stiffness Measurement (CSM) [35,
204 36] under a 70 Hz harmonic oscillation frequency and 2 nm of harmonic amplitude [36]

205 maintaining a constant 0.05 s^{-1} indentation rate. An array of 5×5 indentations distanced 50
206 μm were programmed at a constant 2000 nm depth, calculating the average values between
207 the 400 nm and 600 nm depth to avoid the roughness effect at the initial penetration depth.
208 The reduced elastic modulus (E_r) was calculated instead of the Young's Modulus since the
209 Poisson's coefficient is unknown for these blends and plasticized polymers.

210

211 3. Results and discussion

212 Fig. 1 shows the visual appearance of samples recovered at different testing times. In
213 general terms, all materials increased their opacity during composting even at the first tested
214 time (7 days). It is noticeable that PHB slowed down the PLA disintegration rate, since
215 formulations with PHB were still visible after 28 days, while those with no PHB were
216 completely disintegrated at that time. It was observed that disintegrability under composting
217 started in the polymers amorphous phase and this was mostly attacked by microorganisms at
218 the initial stage of this process. This effect was apparent by the loss of transparency in films
219 after treatment. The increase in crystallinity in all these materials decreased their degradation
220 rate since the ordered structure in the crystalline fractions could retain the action of
221 microorganisms. Thus, the addition of mostly crystalline PHB slowed down the disintegration
222 of the PLA matrix. In fact, in a previous work we studied the disintegrability of neat PHB
223 films in composting conditions and it was observed that it only reached 1.5% after 35 days
224 [5]. On the other hand, the addition of plasticizers resulted in a clear increase in the
225 disintegration phenomenon.

226 Fig. 2 shows the colorimetric results obtained after 7 days of exposition to composting
227 conditions. The characteristic high brightness of neat PLA decreased after 7 days in
228 composting as evidenced by the decrease in the lightness value (L) (Fig. 2a). A similar trend
229 was observed for PLA and PLA-PHB blends plasticized with ATBC. However, a different
230 behaviour was observed for films plasticized with PEG. These samples showed some increase
231 in lightness with testing time. This effect could be due to some plasticizer losses and the
232 consequent compression of macromolecular chains. The addition of PHB to the PLA matrix
233 produced the increase in clear amber tone in PLA-PHB blends. The yellowness index (YI)
234 was measured and results are shown in Fig. 2b. No significant differences in YI were
235 observed between neat and plasticized PLA films before and after 7 testing days. Plasticized
236 PLA/PHB blends showed a clear decrease in YI values, being this effect more evident in the
237 PLA/PHB-PEG film. In addition, positive values of b^* , indicative of a deviation towards

238 yellow, as well as negative values of a^* , indicative of a deviation towards green, corroborated
239 this tendency to color change in PLA/PHB-PEG films (Fig. 2c).

240 As can be seen in Fig. 1 some differences in visual appearance after 7 days of
241 composting with respect to the corresponding formulation before the test start were observed.
242 Total color difference (ΔE) values indicated that neat PLA was the only sample with no
243 apparent visual changes ($\Delta E = 1.7$), since ΔE values higher than 2.0 represent the threshold of
244 the perceptible color difference for the human eye [37]. The ΔE values for PLA-PEG and
245 PLA-ATBC films were 2.9 and 2.5, respectively, while they were 5.3 and 2.1 for PLA/PHB-
246 PEG and PLA/PHB-ATBC, correspondingly. In summary, all plasticized materials showed
247 perceptible color changes after only 7 days of composting treatment. Changes in films color
248 at the first stages of the composting test were related to the beginning of the hydrolytic
249 degradation process, inducing some changes in the films refraction index as a consequence of
250 water absorption and/or the presence of hydrolysis products [33]. At higher testing times,
251 films color could not be determined in the same way due to the samples rupture into small
252 pieces and their irregular surfaces. Nevertheless, some qualitative observations could be
253 drawn, since it was clearly noticeable that apparent color changes were related to the
254 degradation stage. PLA/PHB blends tended to yellow at high testing times (Fig. 1), due to the
255 PLA disintegration and the consequent increase in the PHB proportion in these formulations.
256 Finally, at 28 days, samples showed a clear yellowness pattern due to the total disintegration
257 of the PLA matrix (Fig. 1).

258 Visual observations were confirmed by calculating the disintegration degree (weight
259 loss) as a function of time (Fig. 3) where 90% of disintegration was considered as the goal of
260 samples disintegrability [33], as indicated in the current legislation for biodegradable
261 materials [31]. No significant differences in weight loss were observed between samples after
262 7 days, but after 14 days the disintegration rate clearly increased for all formulations. SEM
263 micrographs (Fig. 4) showed deep fractures on the films surfaces after 7 testing days, and
264 they were particularly notorious in plasticized materials. No significant differences were
265 observed in plasticized PLA/PHB blends, but PLA-PEG showed higher disintegration rate
266 than PLA-ATBC. This significant difference in plasticized PLA films could be explained by
267 the hydrophilic nature of PEG, in contrast with the hydrophobic character of ATBC. Water
268 absorption and diffusion through the polymer bulk in the initial phase of disintegration in
269 PLA-PEG films was faster than in PLA-ATBC, resulting in higher hydrolysis in the polymer
270 chain leading to small molecules (monomers and short-chain oligomers) that are available for
271 the microorganisms attack [26]. However, PLA/PHB-ATBC blends showed higher

272 disintegration rate (up to 65%) after 21 days of composting than PLA/PHB-PEG (below
273 50%). This different behaviour could be explained by the formation of acid groups during the
274 plasticizer release in PLA/PHB-ATBC films, which are able to promote the hydrolysis of
275 polymer chains [33] and consequently accelerating the disintegration process. This result was
276 confirmed by FTIR analysis where the formation of hydroxyl groups ($3200\text{-}3600\text{ cm}^{-1}$) in
277 plasticized PLA-PHB blends showed higher intensity for the PLA/PHB-ATBC blend, as
278 discussed below. Moreover, SEM micrographs of the PLA/PHB-ATBC blend after 21 days in
279 composting conditions also showed evident signs of surface erosion with deep fractures,
280 while the PLA/PHB-PEG blend showed a more regular surface. As observed in Fig.3,
281 plasticized PLA films achieved more than 85% of disintegration after 21 days and all
282 materials showed weight losses higher than 90% after 28 days, indicating the compostable
283 nature of all these blends.

284 The film surfaces were also investigated by optical microscopy and their roughness
285 profiles were determined with the EDF-z technique (Fig. 5). In a previous work we observed
286 that neat PLA films showed smooth surfaces which were rough in neat PHB films [5]. When
287 applying this technique to PLA and plasticized PLA films, smooth surfaces were obtained
288 (Fig. 5) in both cases, although plasticized PLA/PHB films showed some roughness. The
289 more irregular surface profiles showed by films with PHB could be attributed to its higher
290 crystallinity. After 21 days under composting conditions, all samples showed some increase
291 in roughness when compared to the same formulation before the beginning of the test.

292 Fig. 6 shows the FTIR spectra of each film at different testing times. All PLA based
293 samples revealed the typical band at 1750 cm^{-1} assigned to the asymmetric stretching of the
294 carbonyl group (-C=O) by lactide [1, 25]. At 1180 cm^{-1} the -C-O- bond stretching in the -CH-
295 O- group of PLA was also observed [25]. The 1450 cm^{-1} band was assigned to the -CH_3
296 group [1, 38]. It was reported that the intensity of the -C=O band increased with the
297 composting time due to the hydrolytic degradation, resulting in some increase in the number
298 of carboxylic end groups in the polymer chains [25]. In these materials, the -C=O band
299 intensity increased with the composting time in both, PLA and plasticized PLA samples,
300 while it showed broader absorption in films containing PHB. This result was related to the
301 crystalline carbonyl group stretching in PHB at 1735 cm^{-1} [29]. The good miscibility between
302 PLA and PHB was related to the observation of a unique narrow band corresponding to the
303 carbonyl group [9]. Two bands were clearly observed in the PLA/PHB-ATBC film at this
304 wavenumber range at early disintegration stages (Fig. 6e). This observation could be related
305 to some loss of interaction between both polymers with the increase in disintegration time.

306 Another important band was observed around 1600 cm^{-1} , corresponding to the formation of
307 carboxylate ions by the action of microorganisms, able to consume lactic acid and PLA
308 oligomers on the film surface leaving carboxylate ions at the chain ends [33]. This behaviour
309 was particularly noticeable in PLA-ATBC films after 21 days under composting (Fig. 6c). It
310 should be also highlighted that this band appeared after 7 days in PLA and plasticized PLA
311 samples and after 14 days in plasticized PLA/PHB films, confirming that PHB helps to slow
312 down the PLA disintegration rate under composting conditions. Two more bands
313 corresponding to the amorphous and crystalline phases of PLA were observed at 866 cm^{-1}
314 and 756 cm^{-1} , respectively [38]. These bands seemed to be unmodified in all samples during
315 the whole composting test with the exception of the PLA-ATBC film, in which the band at
316 866 cm^{-1} clearly increased in intensity after 21 days (Fig. 6c).

317 TG and DTG curves (not shown) revealed the complete weight loss of PLA and
318 plasticized PLA films in a single degradation step, while plasticized PLA/PHB blends were
319 degraded in two steps, where the first one was assigned to the PHB decomposition and the
320 second one, at higher temperatures, was related to the PLA thermal degradation. The initial
321 degradation temperature (T_0) was calculated for decomposition degree (α) 0.05 and the
322 maximum degradation temperatures (T_{\max}) were calculated from TG and DTG curves. The
323 main results are summarized in Table 1. It was observed that both degradation temperatures
324 decreased significantly with the disintegration time. While a slight decrease (around 0.3%)
325 was observed for T_0 of neat PLA after 7 days, plasticized PLA films showed higher
326 reductions (around 11% in PLA-PEG and 10% in PLA-ATBC). Lower reductions were
327 observed for PLA/PHB-PEG and PLA/PHB-ATBC blends (5% and 1% in T_0 , respectively).
328 The decrease in T_0 after 7 testing days could be related with the high plasticizer loss caused
329 by hydrolysis during the initial disintegration stages. It was also observed that plasticizers
330 were more efficiently retained by PLA/PHB blends than by neat PLA. After 7 days the
331 reduction of T_{\max} in PLA did not show large differences between PLA, PLA-PEG and
332 plasticized PLA/PHB blends (around 3-5%) but PLA-ATBC showed a considerable reduction
333 in this value, close to 20%. The T_{\max} of PLA reached the maximum reduction (18-23%) after
334 21 days in plasticized PLA films. The corresponding peak of DTG associated with the PLA
335 thermal degradation almost disappeared in the PLA/PHB-PEG film after 21 days, suggesting
336 the gradual disappearance of PLA in the blend by being preferentially attacked by
337 microorganisms during composting. Conversely, the reductions of T_{\max} corresponding to the
338 PHB thermal degradation only reached 8% after 21 days of disintegration.

339 Fig. 7a shows the chromatogram obtained after pyrolysis of the PLA/PHB-PEG film
340 before composting. Py-GC/MS analysis of all films showed the typical thermal degradation
341 products of PLA with the characteristic series of signals at $m/z = 56 + (n \times 72)$ attributed to
342 the PLA degradation products [34]. Peaks at retention times 17.5 min and 18.5 min showed
343 highly similar mass spectra for $m/z = 56 + 72$ ($n=1$) where the main fragments were those
344 with $m/z = 32, 43, 45$ and 56 being assigned to mesolactide and (L,D)-lactide [34]. For
345 PLA/PHB blends, the broad peak of crotonic acid showing the main fragmentation at $m/z =$
346 $39, 41, 68, 69,$ and $86,$ was observed [5]. The peak at 23 min retention time was only
347 observed in films plasticized with PEG with $m/z = 32, 41, 68, 87, 103, 154,$ corresponding to
348 the thermal degradation products of PEG. On the other hand, blends plasticized with ATBC
349 showed two main peaks corresponding to tributyl propene-1,2,3-tricarboxylate ($m/z = 41, 57,$
350 $112, 139, 156, 157, 168, 213$ and 269) at 40.5 min and the characteristic peak of tributyl
351 acetylcitrate ($m/z = 29, 41, 57, 129, 139, 157, 185$ and 259) at 42.5 min (Fig 7b and 7c).

352 It was observed that PLA/PHB-ATBC samples before and after 21 days under
353 composting conditions showed the same ratio for these two peaks, while the PLA-ATBC film
354 showed some decrease in the intensity of the tributyl propene-1,2,3-tricarboxylate peak after
355 21 days, suggesting that ATBC was easily released from the PLA matrix. This result is in
356 agreement with the higher degradation rate in PLA-ATBC samples (Fig. 3). This behaviour
357 could be explained by the preferential microorganisms attack to low molar mass fragments,
358 which are more easily consumed when ATBC is available while these molecules are more
359 difficult to reach in the non-plasticized PLA/PHB blend. Furthermore, smaller peaks at higher
360 retention times also showed the characteristic series of signals of PLA ($m/z = 56 + n \times 72$)
361 with $n = 2$ and 3 . Table 2 also shows the mesolactide to (D,L)-lactide ratio obtained from the
362 Py-GC/MS chromatograms. These results showed the increase in the mesolactide fraction of
363 all materials during composting and they could be related to the preferential selection of
364 microorganisms to attack the L-lactide fraction of the polymer structure [39].

365 Nanomechanical properties were investigated with the nanoindentation technique.
366 Only fresh samples (stored at 25°C and 30% RH) and those after 7 disintegration days could
367 be tested, since those after 14 and 21 days were too fragile. The calculated hardness (H) and
368 reduced modulus (E_r) in depth profiles are shown in Fig. 8 Neat PLA showed the highest H
369 and E_r values (around 200 MPa and 3500 MPa, respectively). The presence of either
370 plasticizers or PHB in PLA formulations clearly reduced these parameters, even before the
371 disintegration test, due to the plasticizer effect which reduced the inherent brittleness of both
372 biopolymers [5]. All films after 7 testing days showed lower values than the fresh materials.

373 These results demonstrated that nanoindentation is a powerful tool to evaluate the loss in
374 mechanical properties of biopolymers submitted to composting [40, 41]. The lowest values
375 corresponded to plasticized films after 7 days, corroborating the observation of the higher
376 degradation rate in plasticized materials. Although the reduction on mechanical properties is
377 one of the main consequences of the degradation process occurring during composting, this
378 process also favoured the microorganism's action. This effect could be explained since the
379 loss in mechanical properties after 7 composting days produced a brittle material consisting in
380 broken pieces with a high defects density, such as cracks and porous structure, permitting the
381 easy access of microorganisms to the polymer bulk. The optical inspection of nanoindented
382 samples (Fig. 9) revealed these defects.

383 Fig. 10 shows the H and E_r values averaged between 400 and 600 nm depth for
384 plasticized and unplasticized materials. The reduction in both parameters after 7 composting
385 days was more evident in films plasticized with PEG. While neat PLA lost around 20% in H
386 and E_r , all other materials lost approximately 50%, with the exception of the PLA/PHB-
387 ATBC film that showed a similar behaviour than neat PLA. This result confirmed that ATBC
388 increased the interaction between PLA and PHB and this blend showed higher mechanical
389 resistance.

390

391 **Conclusions**

392 Formulations based on plasticized PLA/PHB blends were successfully disintegrated
393 under composting conditions in less than one month, stating their biodegradable character.
394 The ability of PHB to act as nucleating agent in PLA/PHB blends slowed down the PLA
395 disintegration, while plasticizers speeded it up. TGA analysis revealed that plasticizers were
396 mainly lost during the initial disintegration stages, while substantial losses in mechanical
397 properties for all blends were also observed. The presence of plasticizers favoured the surface
398 hydrolysis leading to the loss in mechanical properties, which also made disintegration easier.
399 Py-GC/MS studies demonstrated the increase in the mesolactide form for all blends due to the
400 high microorganism's activity during composting. In summary, plasticized PLA/PHB blends
401 may offer good perspective for biodegradable food packaging industry by improving the
402 polymer performance in films manufacturing and use.

403

404 **Acknowledgements**

405 Authors thank Spanish Ministry of Economy and Competitiveness by financial support
406 (MAT2011-28468-C02-01 and MAT2011-28468-C02-02). M.P. Arrieta thanks Generalitat

407 Valenciana for Santiago Grisolia Fellowship (2011/007). Authors gratefully acknowledge
408 Prof. M^a Dolores Salvador (Polytechnic University of Valencia) for her assistance with
409 nanomechanical and optical microscope analysis.

410

411 **References**

412 [1] Arrieta MP, López J, Ferrándiz S, Peltzer MA. Characterization of PLA-limonene blends for food
413 packaging applications. *Polymer Testing*. 2013;32:760-8.

414 [2] Auras R, Harte B, Selke S. An Overview of Polylactides as Packaging Materials. *Macromolecular*
415 *Bioscience*. 2004; 4:864.

416 [3] Abdelwahab MA, Flynn A, Chiou B-S, Imam S, Orts W, Chiellini E. Thermal, mechanical and
417 morphological characterization of plasticized PLA-PHB blends. *Polymer Degradation and Stability*.
418 2012;97:1822-8.

419 [4] Fortunati E, Armentano I, Iannoni A, Kenny JM. Development and thermal behaviour of ternary
420 PLA matrix composites. *Polymer Degradation and Stability*. 2010;95:2200-6.

421 [5] Arrieta MP, López J, Hernández A, Rayón E. Ternary PLA-PHB-Limonene blends intended for
422 biodegradable food packaging applications. *European Polymer Journal*. 2014;50:255-70.

423 [6] Bucci DZ, Tavares LBB, Sell I. Biodegradation and physical evaluation of PHB packaging.
424 *Polymer Testing*. 2007;26:908-15.

425 [7] Dong W, Ma P, Wang S, Chen M, Cai X, Zhang Y. Effect of partial crosslinking on morphology
426 and properties of the poly(β -hydroxybutyrate)/poly(d,l-lactic acid) blends. *Polymer Degradation and*
427 *Stability*. 2013;98:1549-55.

428 [8] Furukawa T, Sato H, Murakami R, Zhang JM, Duan YX, Noda I, et al. Structure, dispersibility,
429 and crystallinity of poly(hydroxybutyrate)/poly(L-lactic acid) blends studied by FT-IR
430 microspectroscopy and differential scanning calorimetry. *Macromolecules*. 2005;38:6445-54.

431 [9] Zhang M, Thomas NL. Blending Polylactic Acid with Polyhydroxybutyrate: The Effect on
432 Thermal, Mechanical, and Biodegradation Properties. *Advances in Polymer Technology*. 2011;30:67-
433 79.

434 [10] Bartczak Z, Galeski A, Kowalczyk M, Sobota M, Malinowski R. Tough blends of poly(lactide)
435 and amorphous poly([R,S]-3-hydroxy butyrate) - Morphology and properties. *European Polymer*
436 *Journal*. 2013;49:3630-41.

437 [11] Blümm E, Owen AJ. Miscibility, crystallization and melting of poly(3-hydroxybutyrate)/ poly(l-
438 lactide) blends. *Polymer*. 1995;36:4077-81.

439 [12] Hu Y, Sato H, Zhang J, Noda I, Ozaki Y. Crystallization behavior of poly(l-lactic acid) affected
440 by the addition of a small amount of poly(3-hydroxybutyrate). *Polymer*. 2008;49:4204-10.

441 [13] Zhang L, Xiong C, Deng X. Miscibility, crystallization and morphology of poly(β -
442 hydroxybutyrate)/poly(d,l-lactide) blends. *Polymer*. 1996;37:235-41.

- 443 [14] Focarete ML, Ceccorulli G, Scandola M, Kowalczyk M. Further evidence of crystallinity-induced
444 biodegradation of synthetic atactic poly(3-hydroxybutyrate) by PHB-depolymerase A from
445 *Pseudomonas lemoignei*. Blends of atactic poly(3-hydroxybutyrate) with crystalline polyesters.
446 *Macromolecules*. 1998;31:8485-92.
- 447 [15] Burgos N, Martino VP, Jiménez A. Characterization and ageing study of poly(lactic acid) films
448 plasticized with oligomeric lactic acid. *Polymer Degradation and Stability*. 2013;98:651-8.
- 449 [16] Lemmouchi Y, Murariu M, Dos Santos AM, Amass AJ, Schacht E, Dubois P. Plasticization of
450 poly(lactide) with blends of tributyl citrate and low molecular weight poly(D,L-lactide)-b-
451 poly(ethylene glycol) copolymers. *European Polymer Journal*. 2009;45:2839-48.
- 452 [17] Courgneau C, Domenek S, Guinault A, Averous L, Ducruet V. Analysis of the Structure-
453 Properties Relationships of Different Multiphase Systems Based on Plasticized Poly(Lactic Acid).
454 *Journal of Polymers and the Environment*. 2011;19:362-71.
- 455 [18] Bitinis N, Fortunati E, Verdejo R, Bras J, Kenny JM, Torre L, et al. Poly(lactic acid)/natural
456 rubber/cellulose nanocrystal bionanocomposites. Part II: Properties evaluation. *Carbohydrate*
457 *Polymers*. 2013;96:621-7.
- 458 [19] Erceg M, Kovacic T, Klaric I. Thermal degradation of poly(3-hydroxybutyrate) plasticized with
459 acetyl tributyl citrate. *Polymer Degradation and Stability*. 2005;90:313-8.
- 460 [20] Parra DF, Fusaro J, Gaboardi F, Rosa DS. Influence of poly (ethylene glycol) on the thermal,
461 mechanical, morphological, physical-chemical and biodegradation properties of poly (3-
462 hydroxybutyrate). *Polymer Degradation and Stability*. 2006;91:1954-9.
- 463 [21] Quintana R, Persenaire O, Lemmouchi Y, Sampson J, Martin S, Bonnaud L, et al. Enhancement
464 of cellulose acetate degradation under accelerated weathering by plasticization with eco-friendly
465 plasticizers. *Polymer Degradation and Stability*. 2013;98:1556-62.
- 466 [22] Yagi H, Ninomiya F, Funabashi M, Kunioka M. Thermophilic anaerobic biodegradation test and
467 analysis of eubacteria involved in anaerobic biodegradation of four specified biodegradable polyesters.
468 *Polymer Degradation and Stability*. 2013;98:1182-7.
- 469 [23] Armentano I, Bitinis N, Fortunati E, Mattioli S, Rescignano N, Verdejo R, et al. Multifunctional
470 nanostructured PLA materials for packaging and tissue engineering. *Progress in Polymer Science*.
471 2013;38:1720-47.
- 472 [24] Song JH, Murphy RJ, Narayan R, Davies GBH. Biodegradable and compostable alternatives to
473 conventional plastics. *Philosophical Transactions of the Royal Society B: Biological Sciences*.
474 2009;364:2127-39.
- 475 [25] Fortunati E, Puglia D, Santulli C, Sarasini F, Kenny JM. Biodegradation of Phormium
476 tenax/poly(lactic acid) composites. *Journal of Applied Polymer Science*. 2012;125:E562-E72.
- 477 [26] Kale G, Auras R, Singh SP. Degradation of commercial biodegradable packages under real
478 composting and ambient exposure conditions. *Journal of Polymers and the Environment*. 2006;14:317-
479 34.

- 480 [27] Sarasa J, Gracia JM, Javierre C. Study of the biodisintegration of a bioplastic material waste.
481 *Bioresource Technology*. 2009;100:3764-8.
- 482 [28] Corrêa MCS, Rezende ML, Rosa DS, Agnelli JAM, Nascente PAP. Surface composition and
483 morphology of poly(3-hydroxybutyrate) exposed to biodegradation. *Polymer Testing*. 2008;27:447-52.
- 484 [29] Weng YX, Wang L, Zhang M, Wang XL, Wang YZ. Biodegradation behavior of
485 P(3HB,4HB)/PLA blends in real soil environments. *Polymer Testing*. 2013;32:60-70.
- 486 [30] Martino VP, Ruseckaite RA, Jimenez A. Ageing of poly(lactic acid) films plasticized with
487 commercial polyadipates. *Polymer International*. 2009;58:437-44.
- 488 [31] UNE EN-ISO 20200. Determination of the degree of disintegration of plastic materials under
489 simulated composting conditions in a laboratory-scale test. 2006.
- 490 [32] Martucci JF, Ruseckaite RA. Tensile Properties, Barrier Properties, and Biodegradation in Soil of
491 Compression-Molded Gelatin-Dialdehyde Starch Films. *Journal of Applied Polymer Science*.
492 2009;112:2166-78.
- 493 [33] Fortunati E, Armentano I, Iannoni A, Barbale M, Zaccheo S, Scavone M, et al. New
494 multifunctional poly(lactide acid) composites: Mechanical, antibacterial, and degradation properties.
495 *Journal of Applied Polymer Science*. 2012;124:87-98.
- 496 [34] Arrieta MP, Parres F, López J, Jiménez A. Development of a novel pyrolysis-gas
497 chromatography/mass spectrometry method for the analysis of poly(lactic acid) thermal degradation
498 products. *J Anal Appl Pyrolysis*. 2013;101:150-5.
- 499 [35] Rayón E, Ferrandiz S, Rico MI, López J, Arrieta MP. Microstructure, mechanical and
500 thermogravimetric characterization of cellulosic by-products obtained from the biomass seeds.
501 *International Journal of Food Properties*. 2014;Accepted.
- 502 [36] Rayón E, López J, Arrieta MP. Mechanical characterization of microlaminar structures extracted
503 from cellulosic materials using nanoindentation technique. *Cellulose Chemistry and Technology*.
504 2013;47:345-51.
- 505 [37] Arrieta MP, Peltzer MA, López J, Garrigós MDC, Valente AJM, Jiménez A. Functional
506 properties of sodium and calcium caseinate antimicrobial active films containing carvacrol. *Journal of*
507 *Food Engineering*. 2014;121:94-101.
- 508 [38] Siracusa V, Blanco I, Romani S, Tylewicz U, Rocculi P, Rosa MD. Poly(lactic acid)-modified
509 films for food packaging application: Physical, mechanical, and barrier behavior. *Journal of Applied*
510 *Polymer Science*. 2012;125:E390-E401.
- 511 [39] Khabbaz F, Karlsson S, Albertsson AC. Py-GC/MS an effective technique to characterizing of
512 degradation mechanism of poly (L-lactide) in the different environment. *Journal of Applied Polymer*
513 *Science*. 2000;78:2369-78.
- 514 [40] Giró-Paloma J, Roa JJ, Díez-Pascual AM, Rayón E, Flores A, Martínez M, et al. Depth-sensing
515 indentation applied to polymers: A comparison between standard methods of analysis in relation to the
516 nature of the materials. *European Polymer Journal*. 2013.

517 [41] Roa JJ, Rayon E, Morales M, Segarra M. Contact mechanics at nanometric scale using
518 nanoindentation technique for brittle and ductile materials. Recent Patents on Nanotechnology.
519 2012;6:142-52.

520

521

522

ACCEPTED MANUSCRIPT

523

524

525 **Fig. 1.** Visual aspect of plasticized PLA and PLA-PHB films at different disintegration times

526

527 **Fig. 2.** Colorimetric parameters of plasticized PLA and PLA-PHB films before and after 7
528 days (7d) under composting conditions from the CIELab space: **a)** Lightness (L) values, **b)**
529 yellowness index (YI) and **c)** a^* and b^* coordinates.

530

531 **Fig. 3.** Degree of disintegration of: control PLA film, plasticized PLA and plasticized PLA-
532 PHB films under composting conditions as a function of time.

533

534 **Fig. 4.** SEM observations of neat PLA, plasticized PLA and plasticized PLA-PHB films at
535 different degradation time under composting conditions.

536

537 **Fig. 5.** EDF-z profiles of films before and after 21 days under composting.

538

539 **Fig. 6.** Infrared spectra ($2000-700\text{ cm}^{-1}$) of: a) PLA, b) PLA-PEG, c) PLA-ATBC, d) PLA-
540 PHB-PEG and e) PLA-PHB-ATBC at different disintegration times under composting
541 conditions. f) Infrared spectra ($4000-2500\text{ cm}^{-1}$) of plasticized PLA-PHB blends at day 0 and
542 21.

543

544 **Fig. 7. a)** Chromatogram obtained after pyrolysis of PLA-PHB-PEG.

545 ATBC degradation products obtained after pyrolysis of: **b)** PLA-ATBC and **c)** PLA-PHB-
546 ATBC before and after 21 days composting test.

547

548 **Fig. 8. a)** Hardness and **b)** modulus curves obtained by nanoindentation of fresh films
549 and those after 7 days in composting conditions.

550

551 **Fig. 9.** Optical micrographs of the films surface of fresh films and after 7 composting days.
552 Fresh PLA film shows the imprints of the Berckovich indenter.

553

554 **Fig. 10.** Summary of H and E_r results for each film calculated (400-600 nm) in depth

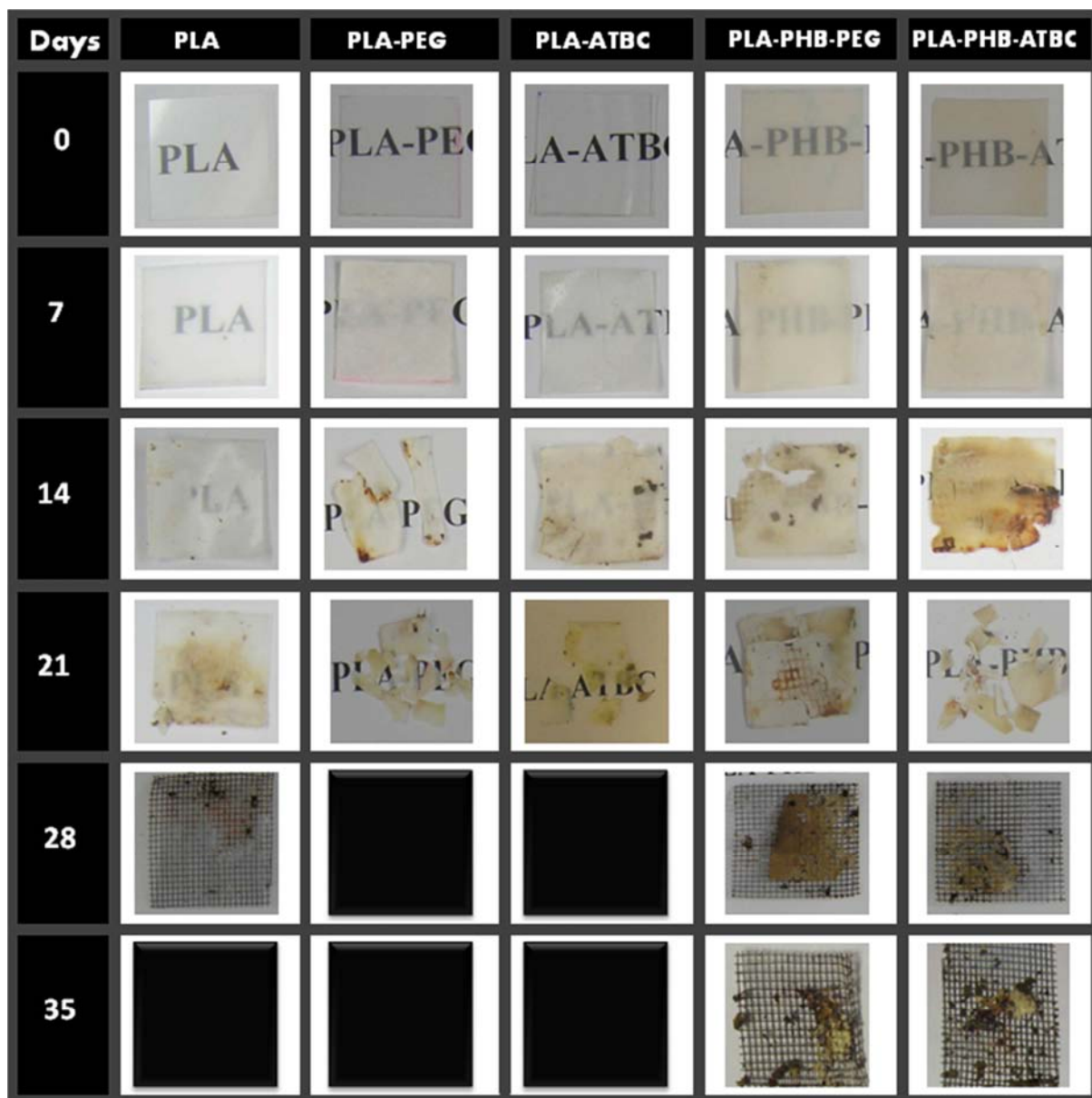
555

Table 1. TG and DTG parameters for films at different disintegration times

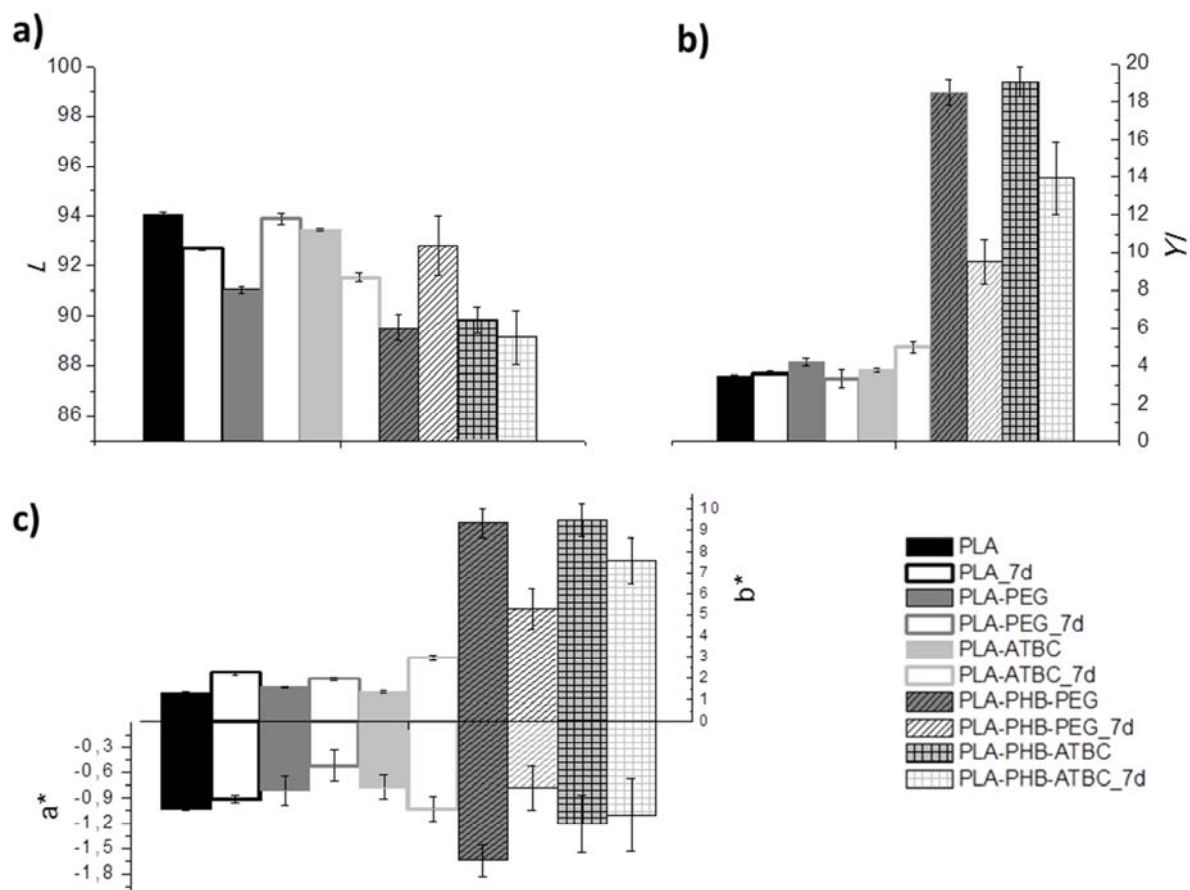
Formulation	Disintegration time (days)	T ₀ (°C)	T _{max} PHB (°C)	T _{max} PLA (°C)
PLA	0	332	-	366
	7	331	-	363
	14	261	-	346
	21	240	-	341
PLA-PEG	0	271		366
	7	240		350
	14	233		325
	21	218		298
PLA-ATBC	0	280		364
	7	253		278
	14	228		291
	21	224		278
PLA-PHB-PEG	0	269	285	324
	7	255	280	314
	14	224	282	337
	21	221	262	-
PLA-PHB-ATBC	0	272	290	361
	7	269	290	346
	14	220	271	332
	21	220	268	285

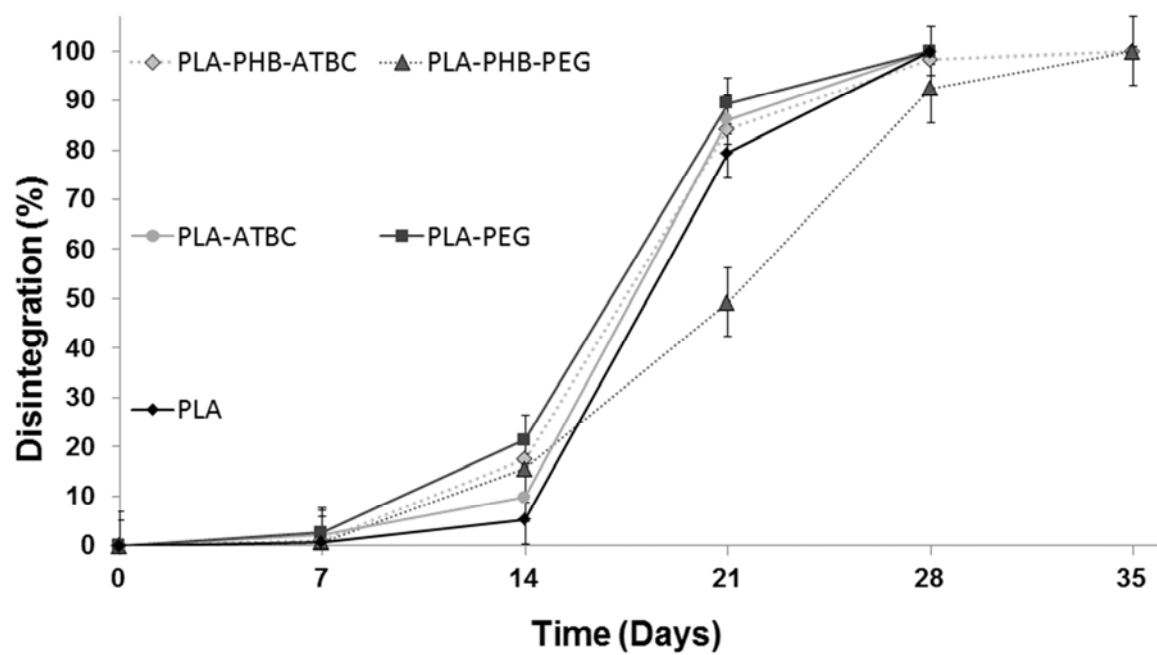
Table 2. Ratio between mesolactide and D,L-Lactide Py-GC/MS areas

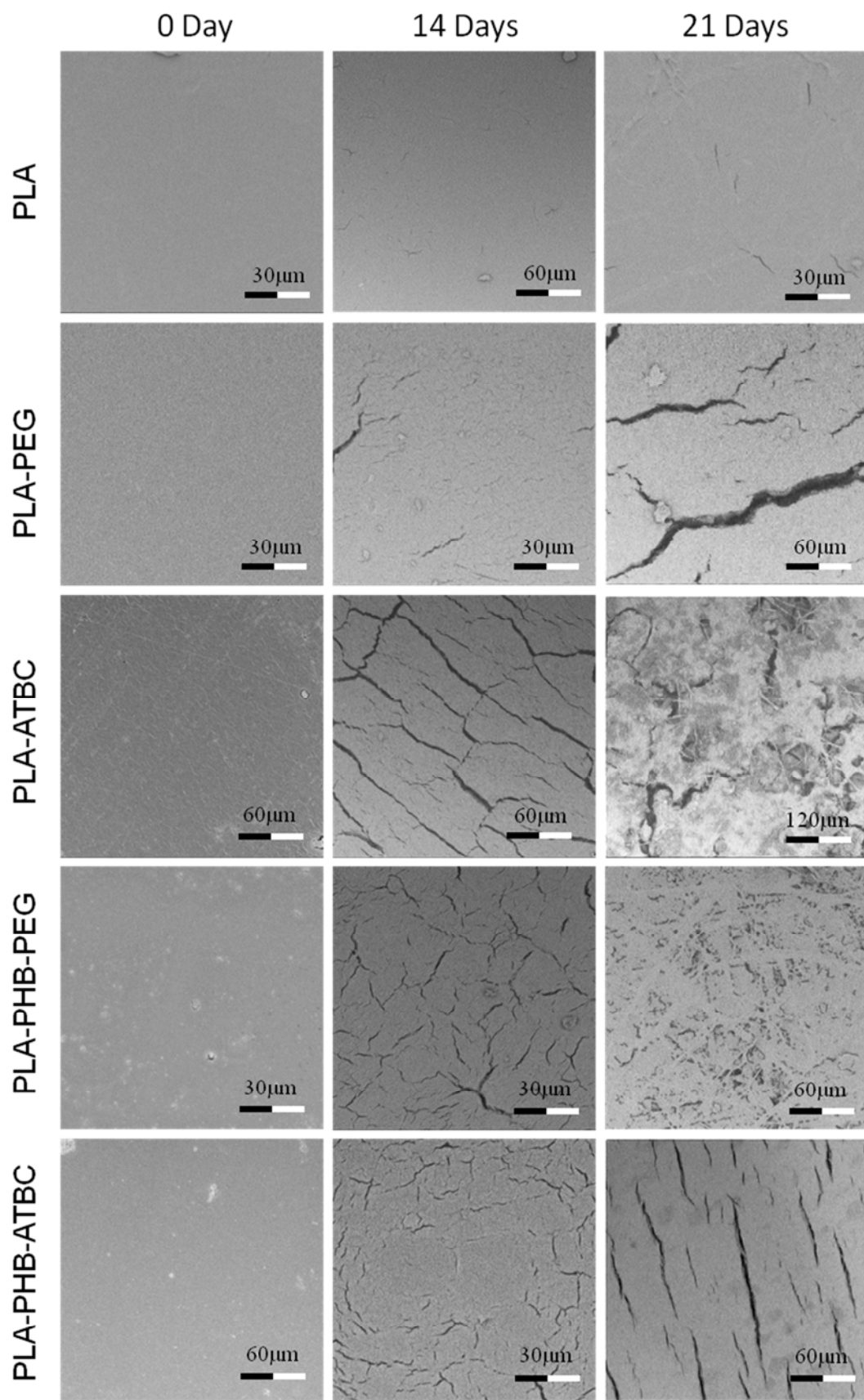
Formulation	Disintegrability day	mesolactide : D,L-Lactide
PLA	0	1 : 3.08
	21	1 : 1.66
PLA-PEG	0	1 : 7.15
	21	1 : 5.61
PLA-ATBC	0	1 : 6.33
	21	1 : 2.47
PLA-PHB	0	1 : 7.86
	21	1 : 2.62
PLA-PHB-PEG	0	1 : 7.36
	21	1 : 5.43
PLA-PHB-ATBC	0	1 : 4.43
	21	1 : 3.39

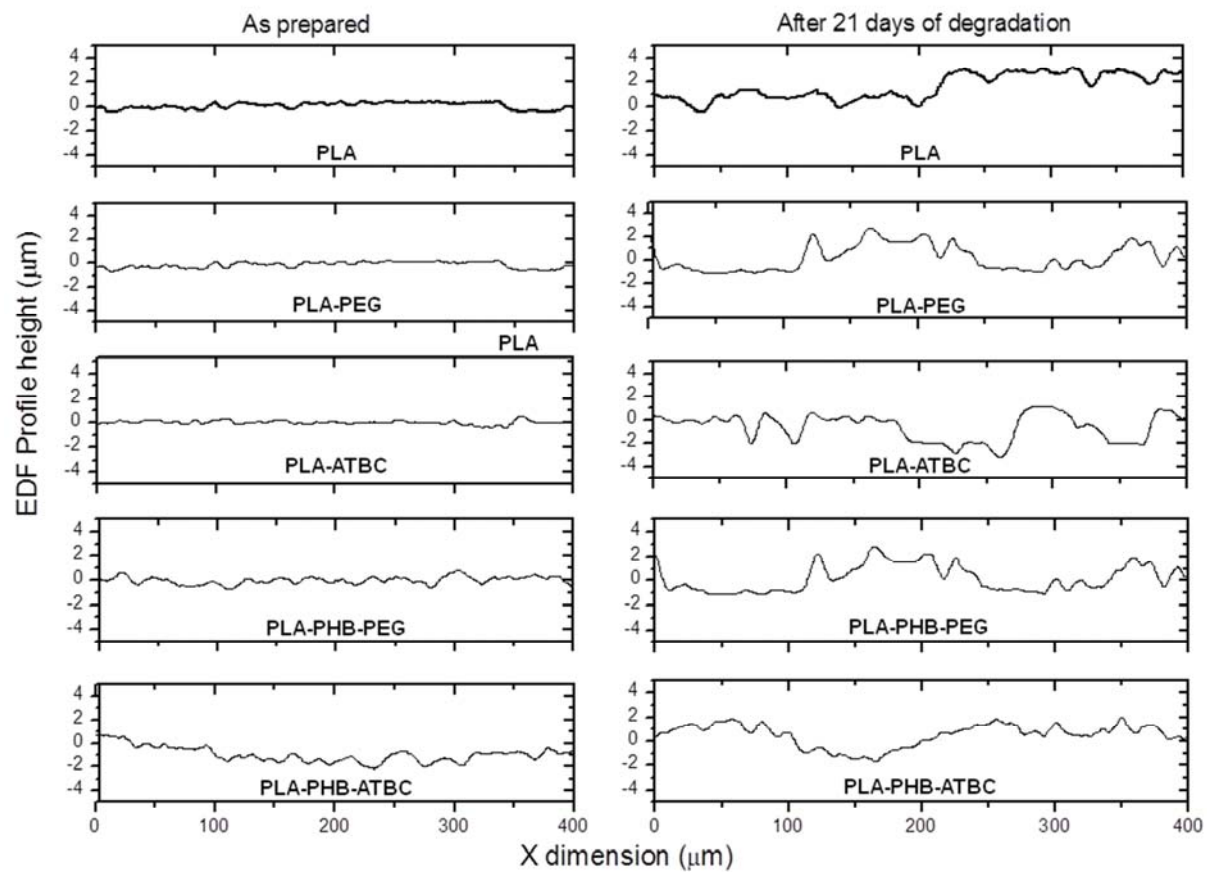


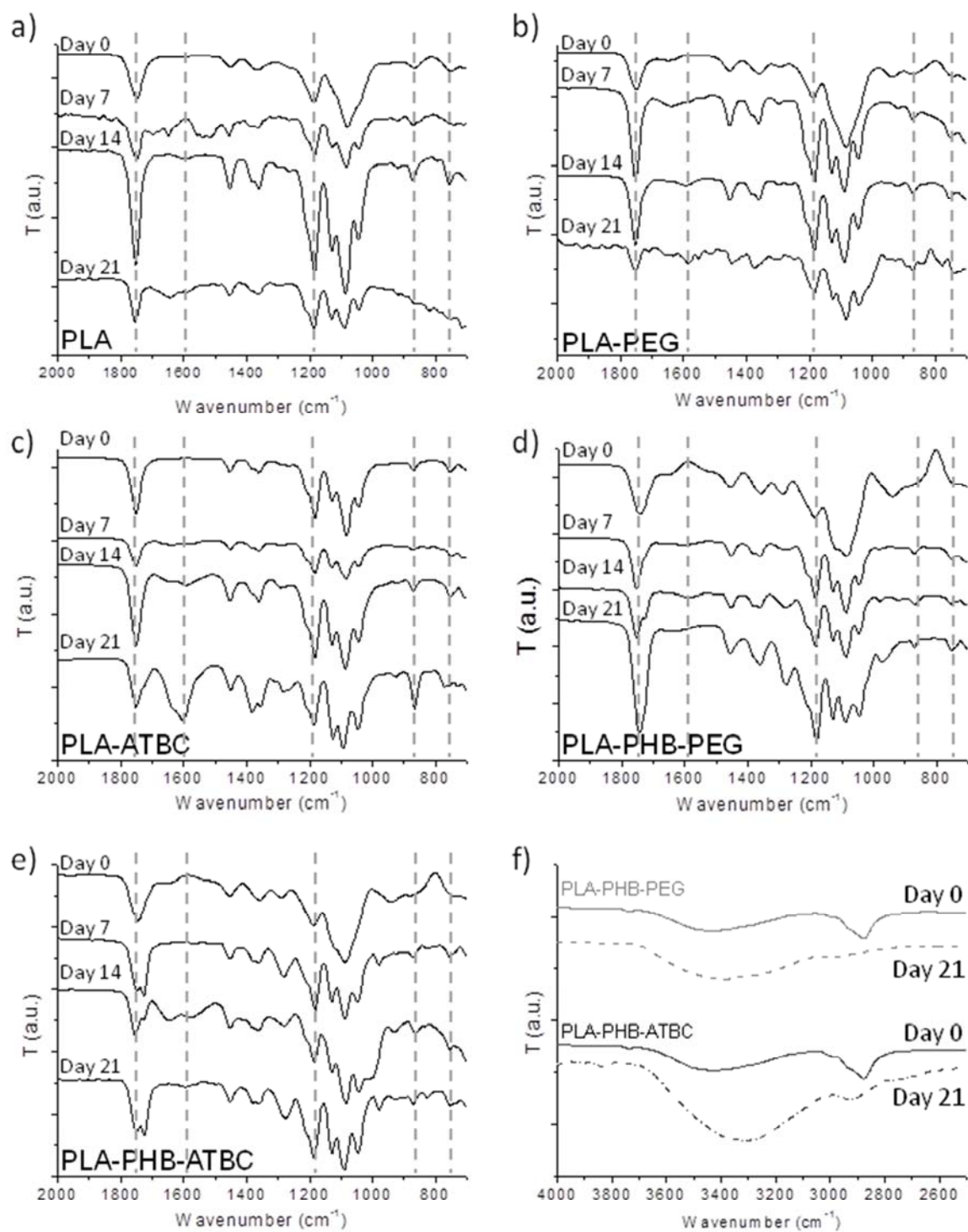
— 10 mm

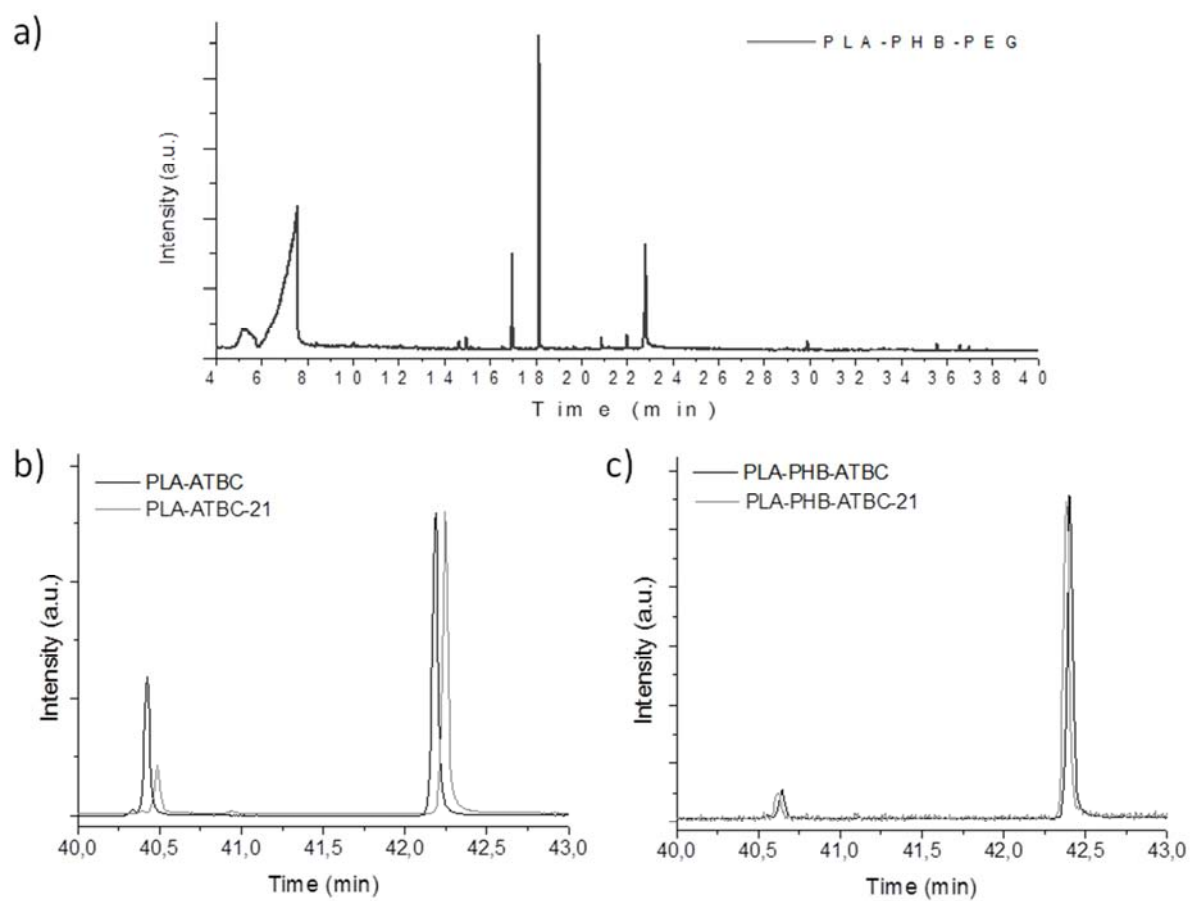


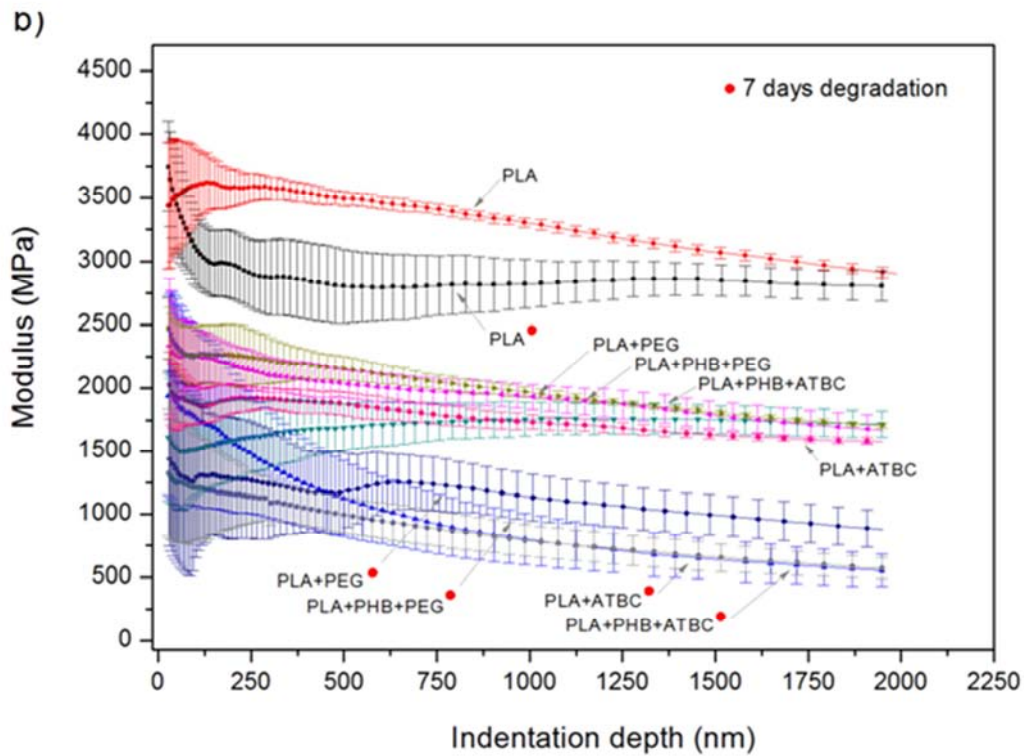
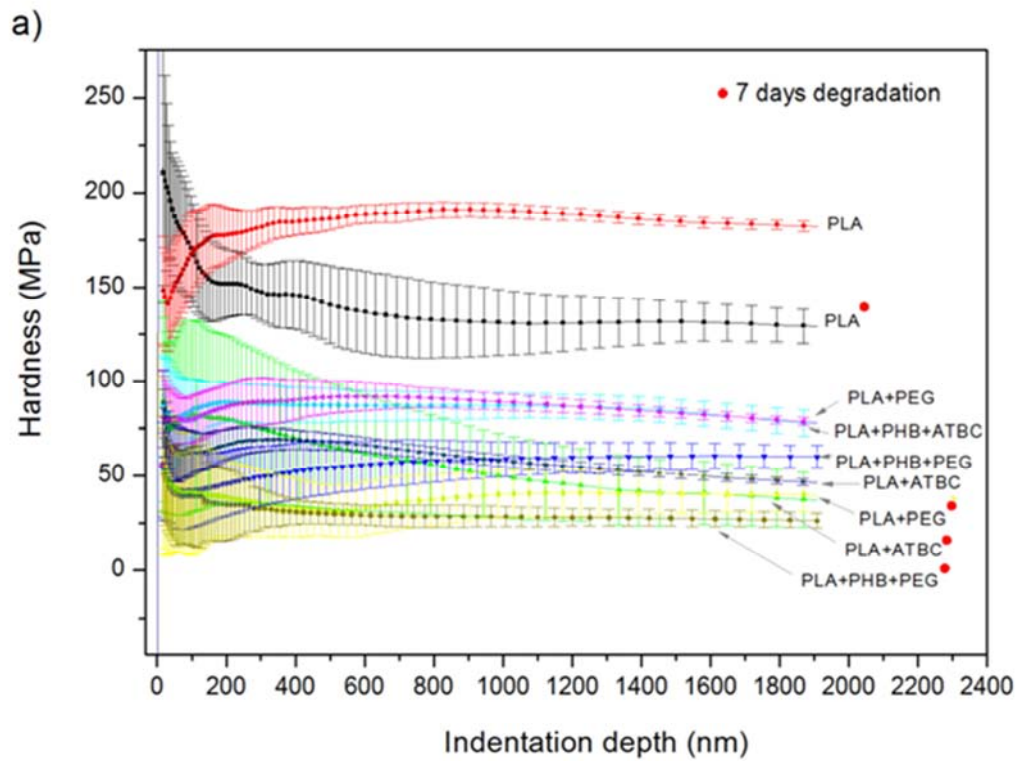


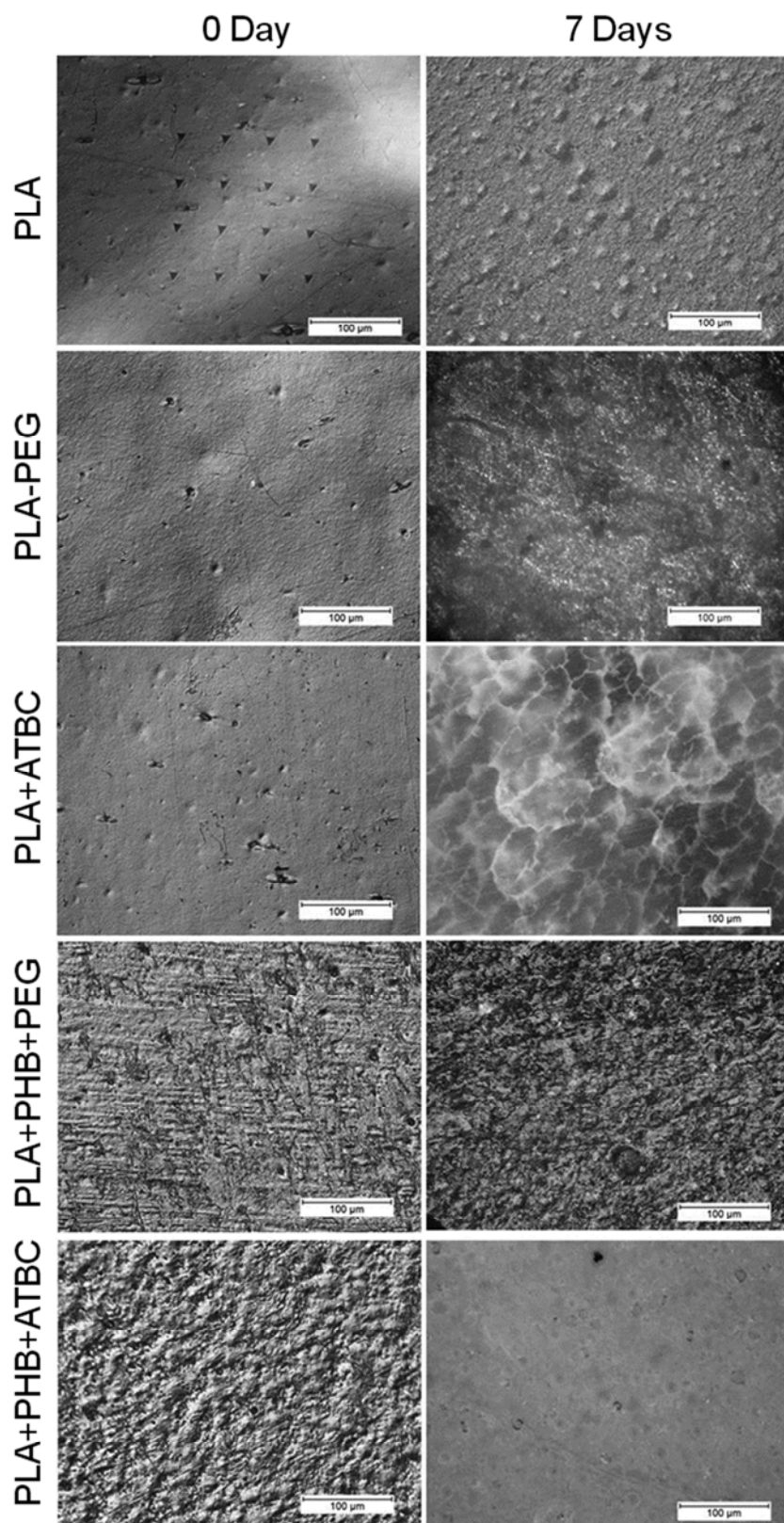












SCRIPT

